OPEN

Correspondence and requests for materials should be addressed to X.W. (xinnanw@ stanford.edu)

PINK1-mediated Phosphorylation of Miro Inhibits Synaptic Growth and Protects Dopaminergic Neurons in *Drosophila*

Pei-I Tsai[1], Meredith M. Course[1,2], Jonathan R. Lovas[1], Chung-Han Hsieh[1], Milos Babic[3], Konrad E. Zinsmaier[4,5] & Xinnan Wang[1]

[1]Department of Neurosurgery, Stanford University School of Medicine, Stanford, CA94304, [2]Neurosciences Program, Stanford University, Stanford, CA94304, [3]Graduate Interdisciplinary Program in Neuroscience, University of Arizona, Tucson, AZ85721, [4]Department of Neuroscience, University of Arizona, Tucson, AZ85721, [5]Department of Molecular and Cellular Biology, University of Arizona, Tucson, AZ85721.

Mutations in the mitochondrial Ser/Thr kinase PINK1 cause Parkinson's disease. One of the substrates of PINK1 is the outer mitochondrial membrane protein Miro, which regulates mitochondrial transport. In this study, we uncovered novel physiological functions of PINK1-mediated phosphorylation of Miro, using *Drosophila* as a model. We replaced endogenous *Drosophila* Miro (DMiro) with transgenically expressed wildtype, or mutant DMiro predicted to resist PINK1-mediated phosphorylation. We found that the expression of phospho-resistant *DMiro* in a *DMiro* null mutant background phenocopied a subset of phenotypes of *PINK1* null. Specifically, phospho-resistant *DMiro* increased mitochondrial movement and synaptic growth at larval neuromuscular junctions, and decreased the number of dopaminergic neurons in adult brains. Therefore, PINK1 may inhibit synaptic growth and protect dopaminergic neurons by phosphorylating DMiro. Furthermore, muscle degeneration, swollen mitochondria and locomotor defects found in *PINK1* null flies were not observed in phospho-resistant *DMiro* flies. Thus, our study established an *in vivo* platform to define functional consequences of PINK1-mediated phosphorylation of its substrates.

M utations in the Ser/Thr kinase PINK1 (PTEN-induced Putative Kinase 1) cause Parkinson's disease (PD), one of the most common neurodegenerative disorders[1]. Emerging evidence suggests that PINK1 functions upstream of another PD-associated protein, the E3 ubiquitin ligase Parkin, to clear damaged mitochondria via mitophagy[2–5]. How PINK1 primes cytosolic Parkin for mitophagy remains unclear, although PINK1-mediated phosphorylation of Parkin or ubiquitin may be involved[6–12]. We have previously shown that PINK1, in cooperation with Parkin, also regulates mitochondrial trafficking by controlling turn-over of Miro[4], an outer mitochondrial membrane (OMM) protein that anchors the kinesin and dynein motors to mitochondria[13–19]. Our work in cultured cells has demonstrated that mitochondrial depolarization or damage stabilizes PINK1 on the OMM. Concomitantly, PINK1 phosphorylates Miro, which then activates proteasomal degradation of Miro in a Parkin-dependent manner and arrests mitochondrial transport. This may serve as a critical step in quarantining damaged mitochondria prior to their degradation via mitophagy. However, the physiological significance of PINK1-mediated phosphorylation of Miro *in vivo* has not yet been determined.

Recent studies have shown that Mitofusin, another OMM protein, is also a common substrate for both PINK1 and Parkin. Mitofusin facilitates mitochondrial fusion, and mitochondrial damage rapidly degrades Mitofusion causing mitochondria to fragment prior to mitophagy[20–26]. PINK1 also phosphorylates the anti-apoptotic protein Bcl-xL on the OMM of depolarized mitochondria, not to regulate mitophagy, but to prevent cell death[27]. In addition to the PINK1 OMM substrates Miro, Mitofusin and Bcl-xL, PINK1 mediates phosphorylation of the mitochondrial chaperon TRAP1 and the Serine protease HtrA2, which are both located in the mitochondrial inter-membrane space[28,29]. This wide range of the potential substrates of PINK1 suggests that it may have multiple cellular functions.

The consensus target sequence for phosphorylation by PINK1 has remained elusive. To date, Miro is the only PINK1 mitochondrial substrate whose phosphorylation residues have been determined[4]. Two *Drosophila* Miro

(DMiro) peptides with a high degree of similarity to the human sequence were identified as potential targets of PINK1-mediated phosphorylation *in vitro*. In this study, we determined the critical role of PINK1 phosphorylation sites on DMiro for maintaining neuronal homeostasis and protecting dopaminergic (DA) neurons *in vivo*.

Results

Ser182, Ser324, and Thr325 in DMiro Mediate PINK1/Parkin-Dependent Degradation. Six Ser/Thr sites in two DMiro phospho-peptides were identified as potential targets of PINK1-mediated phosphorylation by *in vitro* PINK1 kinase assay and mass spectrometry[4]. We individually substituted each of the six potential phosphorylation sites in DMiro (Ser177, Ser182, Ser323, Ser324, Thr325, or Ser328) with alanine mimicking dephosphorylated DMiro. We determined whether these genetic alterations influenced the excessive degradation of DMiro induced by Parkin co-overexpression in HEK293T cells. Only

DMiroSer182Ala significantly suppressed the loss of DMiro in response to overexpressed Parkin (Figure 1A, B), suggesting that DMiroSer182 is a vital site for PINK1-mediated phosphorylation. DMiroSer182 is analogous to human MiroSer156, which is a major PINK1 phosphorylation site for regulating Miro degradation and mitochondrial motility in cultured cells[4]. Thus, human and *Drosophila* Miro are likely to be regulated by PINK1 in a similar fashion. To test whether any of the other identified potential phospho-sites of DMiro may play a redundant but cooperative role for Parkin-mediated degradation of DMiro, we generated double mutations in DMiro (first phospho-peptide S177A, S182A; second phospho-peptide S324A, T325A) and a triple mutant with all three conserved sites to human Miro changed to alanine (DMiro^S182A,S324A,T325A). All double and triple mutant DMiro showed significant protection (Figure 1A, B). Notably, DMiro^S177A,S182A displayed significantly more resistance to Parkin-triggered degradation than DMiro^S177A did (Figure 1A, B), supporting the hypothesis that DMiroSer182 is a critical site for PINK1-mediated
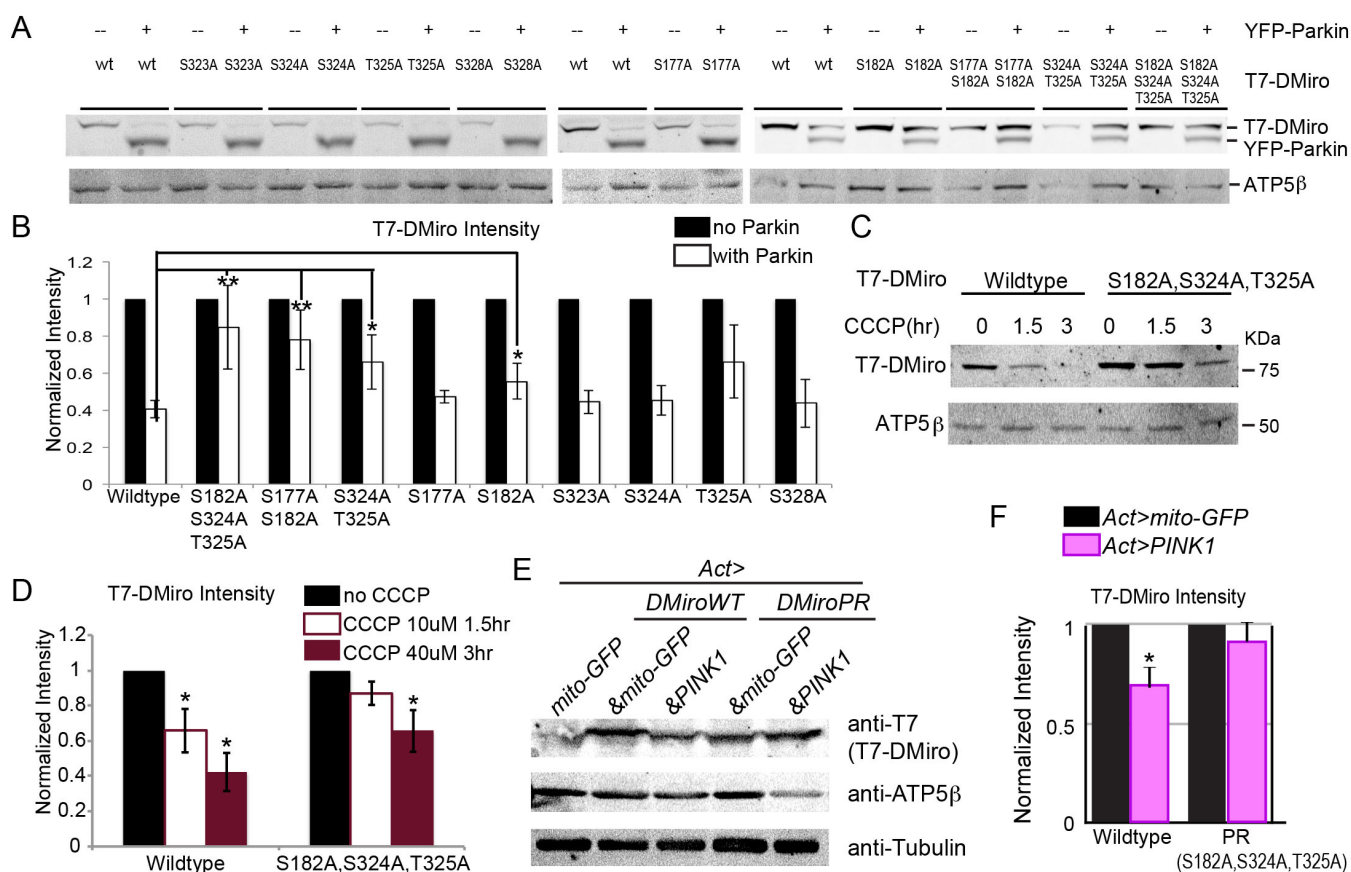
Figure 1 | Ser182, Ser324, and Thr325 of DMiro Mediate PINK1/Parkin-dependent Degradation. (*A*) After transfection with wildtype or mutated forms of T7-DMiro and YFP-Parkin, HEK293T cell lysates were prepared and immunoprobed with anti-T7, anti-ATP5β and anti-GFP. The intensity of each T7-DMiro band was detected with a fluorescence scanner for quantification (*B*) after normalization to the mitochondrial matrix loading control ATP5β, and the control band without Parkin coexpression was set as 1. n = 5–25 transfections. The amounts of overexpressed YFP-Parkin did not significantly vary among different genotypes: P = 0.998 for normalized YFP-Parkin intensity to ATP5β (One-way ANOVA, n = 4 transfections). (*C, D*) HEK293T cells transfected with T7-DMiro were incubated with 10 μM CCCP for 1.5 hr, or 40 μM CCCP for 3 hr, prior to lysing the cells. Immunoblots of lysates were probed with anti-T7, and detected with a fluorescent scanner for quantification (*D*) after normalization to the mitochondrial loading control ATP5β and expressed as a fraction of the control value with no CCCP treatment in the same genotype. n = 4 transfections. 1–2 μg DNA of T7-DMiro and 2 μg of YFP-Parkin were expressed in (*A, B*), and 0.5–1 μg DNA of T7-DMiro was expressed in (*C, D*), in one well of a 6-well plate. (*E*) Lysates from 5 adult flies 5 days after eclosion were analyzed by immunoblotting as indicated. (*F*) The band intensity of T7-DMiro with PINK1 co-expression was normalized to that of ATP5β, and expressed as a fraction of the control value with mito-GFP co-expression. n = 3 independent experiments. ***Act > mito-GFP***: UAS-mito-GFP;Actin-GAL4. ***Act > T7-DMiroWT&mito-GFP***: UAS-mito-GFP,UAS-T7-DMiro^wildtype;Actin-GAL4. ***Act > T7-DMiroPR&mito-GFP***: UAS-mito-GFP,UAS-T7-DMiro^S182A,S324A,T325A;Actin-GAL4. ***Act > T7-DMiroWT&PINK1***: UAS-PINK1,UAS-T7-DMiro^wildtype;Actin-GAL4. ***Act > T7-DMiroPR&PINK1***: UAS-PINK1,UAS-T7-DMiro^S182A,S324A,T325A;Actin-GAL4. * P < 0.05, ** P < 0.01, *** P < 0.001, error bars represent mean ± S.E.M. here and for all figures unless otherwise stated. Uncropped blots are in the supplementary figure.

phosphorylation. We found that the triple mutant DMiro provided the best protection: Parkin overexpression degraded about 60% of co-expressed wildtype DMiro, whereas it only degraded about 20% of DMiro^{S182A,S324A,T325A} (Figure 1A, B). We therefore concluded that Ser182, Ser324, and Thr325 in DMiro mediate PINK1/Parkin-dependent degradation of DMiro.

The PINK1/Parkin pathway is activated by mitochondrial depolarization. To determine if DMiro^{S182A,S324A,T325A} is resistant to depolarization-induced degradation, we applied the mitochondrial uncoupler carbonyl cyanide m-chlorophenyl hydrazone (CCCP) to HEK293T cells transfected with either wildtype or with mutant DMiro. DMiro^{S182A,S324A,T325A} was resistant to CCCP-triggered degradation by mild treatment (10 µM for 1.5 hr), but was still significantly degraded by harsh treatment (40 µM for 3 hr). Mitophagy had not been initiated under either condition since the mitochondrial matrix protein ATP5β was intact (Figure 1C, D).

We next determined whether DMiro^{S182A,S324A,T325A} protected DMiro from PINK1/Parkin-dependent degradation in vivo. We generated transgenic flies bearing T7-tagged wildtype DMiro or DMiro^{S182A,S324A,T325A} downstream of a UAS sequence, using the PhiC31 integrase-mediated transgenesis system to enable same-site insertions in the genome of both transgenes. T7-tagged either wildtype DMiro or DMiro^{S182A,S324A,T325A} was then expressed in flies using the UAS/GAL4 system driven by the ubiquitous driver Actin-GAL4,

with coexpression of UAS-PINK1 or an inert control UAS-mito-GFP. We found that PINK1 rather than mito-GFP overexpression significantly degraded T7-DMiro^{wildtype}, but not T7-DMiro^{S182A,S324A,T325A} in adult fly whole body lysates using western blotting (Figure 1E, F), suggesting that these mutations render DMiro resistance to PINK1-triggered degradation in vivo. This is consistent with the significance of Ser182, Ser324, and Thr325 in mediating PINK1/Parkin-dependent degradation of DMiro in cultured cells (Figure 1A–D).

Generation of a Fly Model Expressing DMiro^{S182A,S324A,T325A} in a DMiro null background. We next introduced the transgene of T7-DMiro^{wildtype} or T7-DMiro^{S182A,S324A,T325A} into a DMiro null background using the UAS/GAL4 system ("DMiro^{null}, da > DMiro^{wildtype}" or "DMiro^{null}, da > DMiro^{S182A,S324A,T325A}" respectively). We found that ubiquitous expression of either transgene rescued the lethality of DMiro null flies as well as the slimness of their third instar larvae (Figure 2A) thus allowing adult survivors, suggesting that both transgenes can restore the essential functions of DMiro. Ubiquitously expressed T7-tagged DMiro^{wildtype} or DMiro^{S182A,S324A,T325A} protein in the DMiro null background was detected from adult fly whole body lysates by western blotting either with anti-T7 or anti-DMiro, and their protein levels did not dramatically differ (Figure 2B). DMiro null third instar larvae had smaller body wall muscle size which was rescued by either
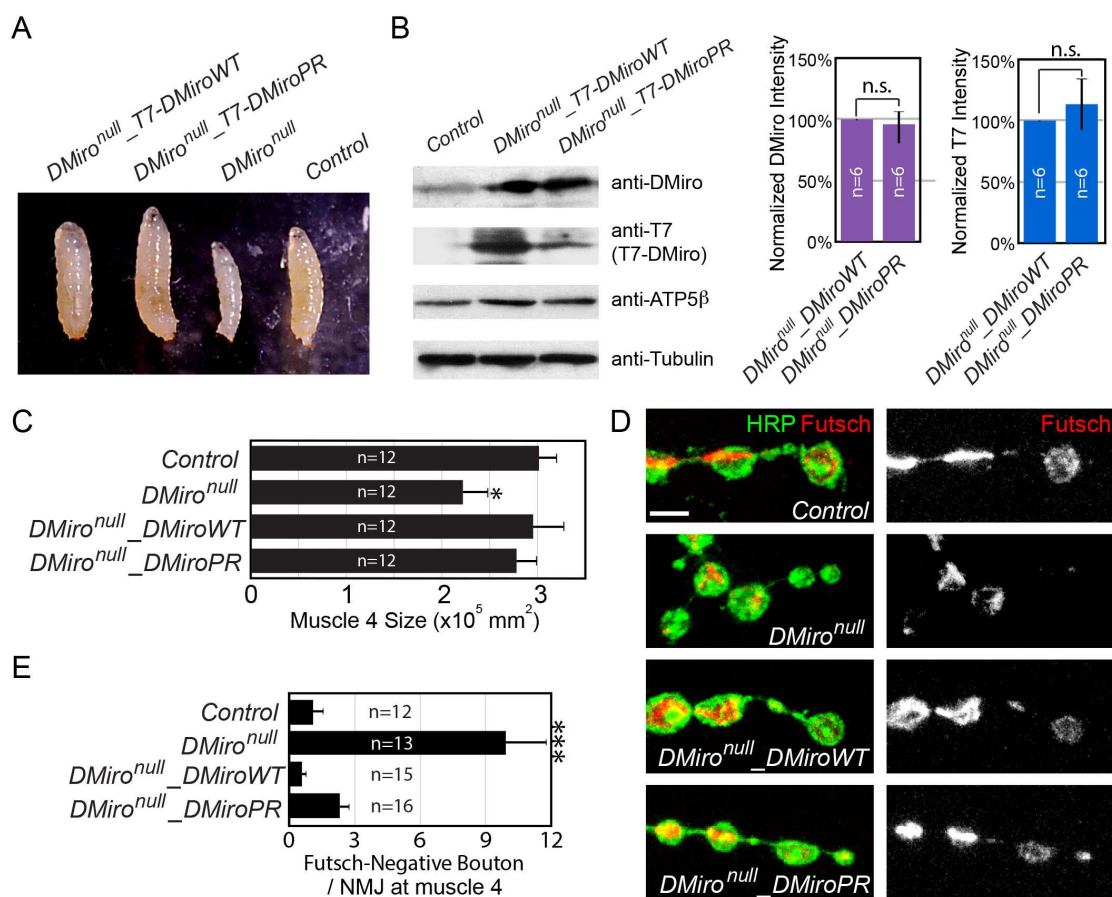
Figure 2 | Generation of a Fly Model Expressing DMiro^{S182A,S324A,T325A} in a DMiro Null Background. (A) Comparison of third instar larval sizes. (B) Lysates from 5 adult flies 5 days after eclosion were analyzed by immunoblotting as indicated. The band intensity recognized by anti-DMiro or anti-T7 was normalized to that of tubulin, and expressed as a percentage of the value of "DMiro^{null}_DMiroWT" and averaged. n = 6 independent experiments. (C) Quantification of muscle 4 size at hemisegment A2. n = 12 third instar larvae. (D) NMJ boutons visualized by anti-HRP (green) and anti-Futsch (red) at muscle 4 hemisegment A2 of third instar larvae. (E) Quantification of the number of Futsch-negative boutons at muscle 4 shown in (D). n = 12–16 larvae. Scale bar: 20 µm. Genotypes used in this figure and the subsequent figures: **Control**: Canton S. **DMiro^{null}**: DMiro^{sd32}/DMiro^{sd26} [16]. **DMiro^{null}_DMiroWT**: UAS-T7-DMiro^{wildtype};da-GAL4_DMiro^{sd32}/DMiro^{sd26}. **DMiro^{null}_DMiroPR**: UAS-T7-DMiro^{S182A,S324A,T325A};da-GAL4_DMiro^{sd32}/DMiro^{sd26}. n.s.: not significant. Comparisons with Control except where otherwise indicated here and for all the following figures.
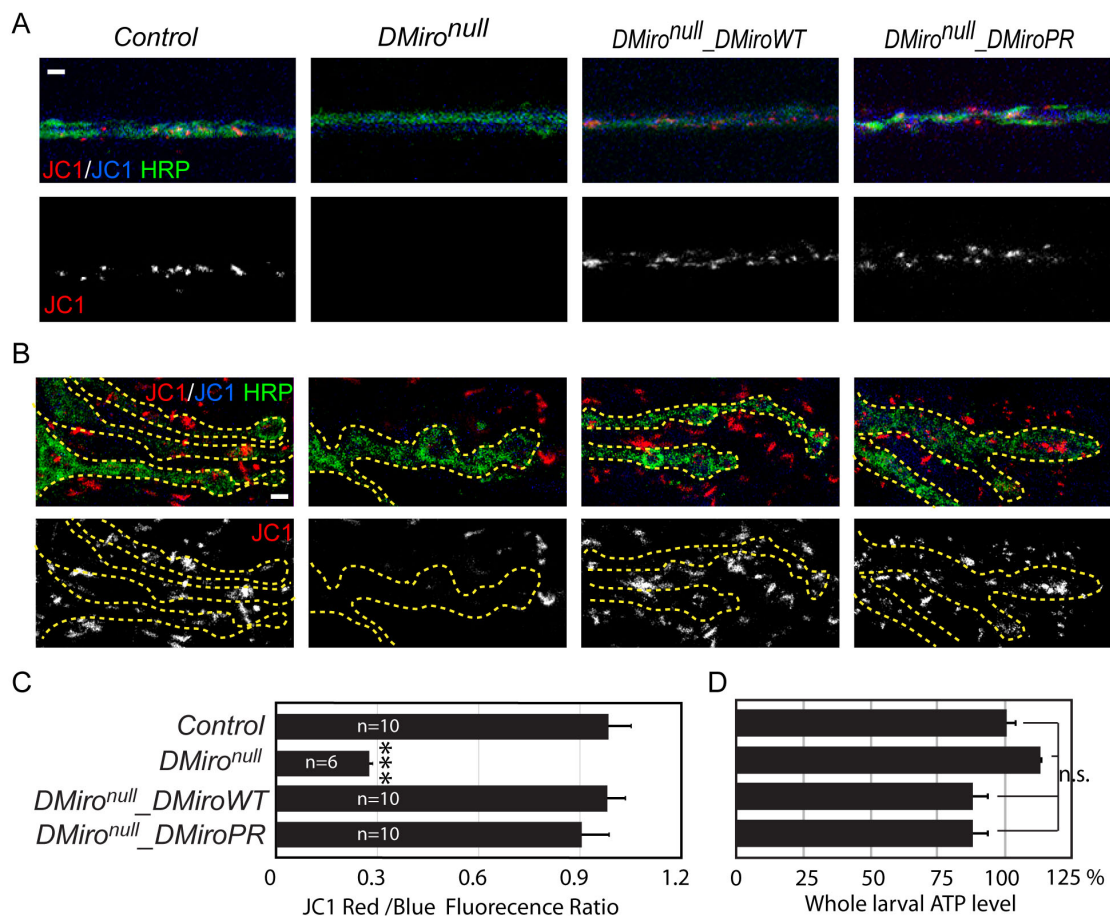
DMiro[wildtype] or by DMiro[S182A,S324A,T325A] (Figure 2C). Loss of the presynaptic microtubule-associated protein Futsch at terminal boutons of *DMiro* null larval neuromuscular junctions (NMJs) was also rescued by either transgene (Figure 2D, E), indicating that Ser182, Ser324, and Thr325 in DMiro do not participate in maintaining Futsch stability.

To examine mitochondrial phenotypes, we first live imaged mitochondria of semi-dissected third instar larvae stained with JC1, a mitochondrial membrane potential-dependent dye. It has been reported that in neurons deficient in endogenous DMiro, mitochondria fail to be recruited to the kinesin motors and microtubules, and thus fail to be transported into axons and synaptic boutons[16]. We observed this phenotype in *DMiro* null where JC1-labeled mitochondria were absent from axons and presynaptic boutons (Figure 3A, B). This phenotype was rescued by expression of either DMiro[wildtype] or by DMiro[S182A,S324A,T325A]. JC1-labeled mitochondria were present in axons and presynaptic boutons of "*DMiro*[null], *da* > *DMiro*[wildtype]" and "*DMiro*[null], *da* > *DMiro*[S182A,S324A,T325A]" (Figure 3A, B), suggesting that these mutations in DMiro do not affect its ability to anchor mitochondria to motors. Axonal mitochondrial JC1 intensity was indistinguishable among control, "*DMiro*[null], *da* > *DMiro*[wildtype]" and "*DMiro*[null], *da* > *DMiro*[S182A,S324A,T325A]" larvae (Figure 3A, C), and therefore these mutations in DMiro do not obviously depolarize

mitochondrial membrane potential. Consistently, ATP levels in third instar larvae were not significantly affected by these mutations (Figure 3D).

DMiro[S182A,S324A,T325A] or Loss of PINK1 Increases Mitochondrial Movement. It has been shown that in axons of third instar larvae with *PINK1* RNAi, mitochondrial motility is increased[4,30]. If this is due to decreased phosphorylation on DMiro, DMiro[S182A,S324A,T325A] should also enhance mitochondrial movement in neurons. To test this hypothesis, we first live recorded mitochondrial movement labeled by accumulative JC1 at NMJs. At controls or at "*DMiro*[null], *da* > *DMiro*[wildtype]" NMJs, mitochondria were mostly static during a 20-second recording; in contrast, at "*DMiro*[null], *da* > *DMiro*[S182A,S324A,T325A]" or at *PINK1* null NMJs, mitochondria underwent dynamic changes in their positions and shapes: significantly more mitochondria shifted in various directions during the recording (Figure 4A, B). Therefore, DMiro[S182A,S324A,T325A] or loss of PINK1 increased mitochondrial movement at NMJs *in vivo*. We next live recorded axonal mitochondrial movement labeled by mito-GFP in neuropeptidergic neurons driven by CCAP-GAL4[4]. Heterozygous *DMiro* null mutations ("+/*DMiro*[null]") allowed mitochondria to be transported into axons (Figure 4C). We thus used "+/*DMiro*[null]" as

Figure 3 | Both Wildtype DMiro and DMiro[S182A,S324A,T325A] Rescue Mitochondrial Phenotypes of *DMiro*[null]. (A) Representative single-section confocal images of JC1 and anti-HRP staining in distal axons close to NMJs passing segment A3 of third instar larvae, red representing accumulative JC1 in mitochondria and blue representing cytoplasmic diffuse JC1. The neuronal membrane marker HRP is in green. (B) Representative single-section confocal images of JC1 and anti-HRP staining at NMJs of muscle 4 hemisegment A3 of third instar larvae. The red mitochondrial JC1 staining in *DMiro*[null] indicates mitochondria present in muscle cells. (C) Quantification of the ratio of JC1 red/blue fluorescent intensity in axons shown in (A). n = 6–10 larvae. The blue intensity was not significantly different among 4 genotypes (P = 0.2598, One-way ANOVA). (D) Quantification of total ATP levels in third instar larvae with indicated genotypes, expressed as a percentage of the control value. n = 5 larvae for each experiment and total 3 independent experiments. Scale bars: 10 μm.
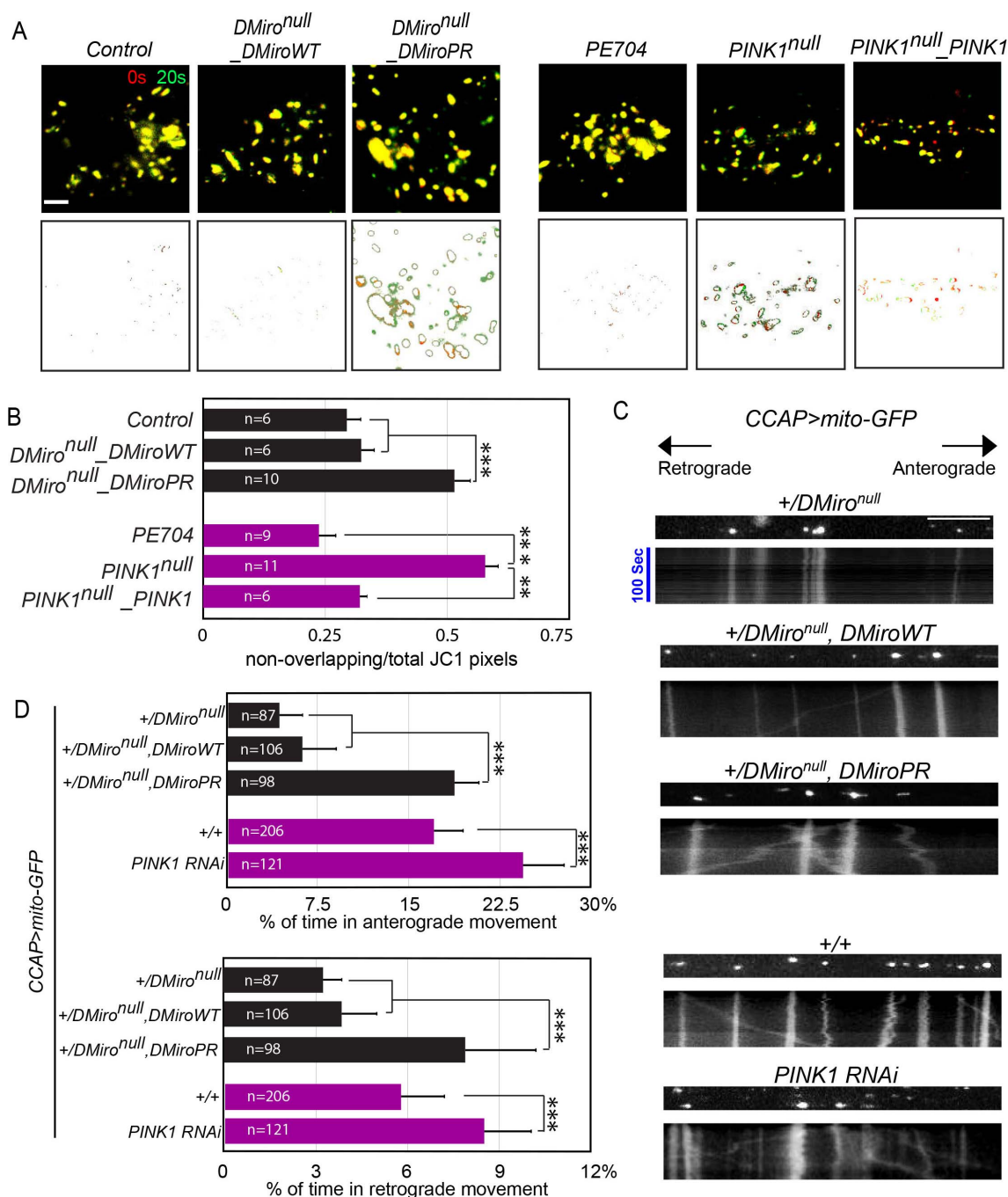
Figure 4 | DMiro^{S182A,S324A,T325A} or Loss of PINK1 Increases Mitochondrial Movement. (A) Representative red/green overlay of two time-lapse images (Δ = 20 s) of accumulative JC1 staining in mitochondria at NMJs of muscle 6/7 hemisegment A3 of third instar larvae. Lower panels extract pixels that are present in only one image. (B) Quantification of the area of non-overlapping pixels between the two overlay images as shown in (A) divided by the total area of JC1 staining in each overlay image. n = 6–11 larvae. (C) Mitochondrial movement labeled by mito-GFP driven by CCAP-GAL4 in representative axons passing segment A3. The first frame of each live-imaging series is shown above a kymograph generated from the movie. The x axis of each is mitochondrial position and the y axis corresponds to time (moving from top to bottom). Vertical white lines represent stationary mitochondria and diagonal lines are moving mitochondria. (D) From kymographs as in (C), the percent of time each mitochondrion in motion was determined and averaged. n = 87–206 mitochondria from 8–12 axons and 5 animals. Scale bars: (A) 5 μm; (C) 10 μm. **PINK1^{null}**: PINK^5/Y^{31}. **PE704**: precise excision control males for PINK1 null[31]. **PINK1^{null}_PINK1**: PINK^5/Y;+;da-GAL4_UAS-PINK1 (males of a rescue control for PINK1 null).

a control background, and found that mitochondrial motility in axons passing segment A3 was significantly increased in "+/DMiro^{null}, UAS-DMiro^{S182A,S324A,T325A}", as compared with "+/DMiro^{null}, UAS-DMiro^{wildtype}" and "+/DMiro^{null}" (Figure 4C, D). As reported previously[4,30], PINK1 RNAi also increased axonal mitochondrial motility (Figure 4C, D). This consistently suggests that a lack of PINK1-mediated phosphorylation of

DMiro^{S182A,S324A,T325A} enhances mitochondrial movement both inside proximal axons and at axonal terminals.

DMiro^{S182A,S324A,T325A} or Loss of PINK1 Causes Synaptic Overgrowth at NMJs. In DMiro null third instar larvae, synaptic boutons appeared abnormal. Some boutons tended to aggregate, causing a cauliflower-like or satellite-like structure[16]. Additionally,

the number of synaptic boutons was significantly increased to about three-fold that of control at muscle 4 or to about two-fold that of control at muscle 6/7 hemisegment A2 (Figure 5A, B). Ubiquitous expression of either DMiro^{wildtype} or DMiro^{S182A,S324A,T325A} rescued the phenotypes of satellite boutons; however, only DMiro^{wildtype} but not DMiro^{S182A,S324A,T325A} significantly reduced the synaptic bouton number to control level (Figure 5A, B). Therefore, bouton organization and number are regulated through distinct domains of DMiro. Importantly, synaptic overgrowth, rather than satellite boutons, was also found in PINK1 null third instar larval NMJs (Figure 5A, B). Collectively, DMiro^{S182A,S324A,T325A} did not affect synaptic bouton organization, but caused synaptic overgrowth which is likely due to failure of PINK1 to phosphorylate Ser182, Ser324, and Thr325.

DMiro^{S182A,S324A,T325A} Causes DA Neurodegeneration in Adult Brains. DA neurodegeneration in the substantia nigra is a hallmark of PD pathology, and loss of DA neurons has been reported in a few alleles that disrupt PINK1 gene expression in Drosophila[32,33]. Intriguingly, PINK1 has been shown to genetically interact with DMiro in Drosophila DA neurons[30]. To explore the possibility that failure of PINK1 to phosphorylate DMiro contributes to DA neuronal loss, we immunostained whole-mount adult brains with anti-TH (tyrosine hydroylase) and counted DA

neurons of control, "DMiro^{null}, da > DMiro^{wildtype}" and "DMiro^{null}, da > DMiro^{S182A,S324A,T325A}", 5 and 15 days after eclosion. We discovered that 15-day old but not 5-day old "DMiro^{null}, da > DMiro^{S182A,S324A,T325A}" flies exhibited a significant reduction in the DA neuron number in the PPL1 (protocerebral posterior lateral 1) cluster (Figure 5C, D), a particular DA neuronal group where age-dependent DA neurodegeneration usually occurs in fly brains bearing PINK1 null or RNAi alleles[32,33], as well as in another DA neuronal group PPL2 (Figure 5C, D). This resemblance in DA neurodegeneration between PINK1 null and "DMiro^{null}, da > DMiro^{S182A,S324A,T325A}", suggests that PINK1-mediated phosphorylation of DMiro plays a critical role in protecting DA neurons in adult brains.

It has been reported that loss of PINK1 causes extensive behavioral phenotypes in adult flies, such as defects in jumping, climbing and flying[31–33]. We found that PINK1 null third instar larvae also had diminished locomotor ability (Figure 6A, B). In contrast, third instar larvae and adult flies of "DMiro^{null}, da > DMiro^{wildtype}" and "DMiro^{null}, da > DMiro^{S182A,S324A,T325A}" were not impaired in loco-motor and flight abilities (Figure 6). Furthermore, we did not observe the prominent phenotypes of muscle degeneration and swollen mito-chondria with fragmented cristae found in PINK1 null adult fly thoraces, in either "DMiro^{null}, da > DMiro^{wildtype}" or "DMiro^{null}, da > DMiro^{S182A,S324A,T325A}" (Figure 7A, B).
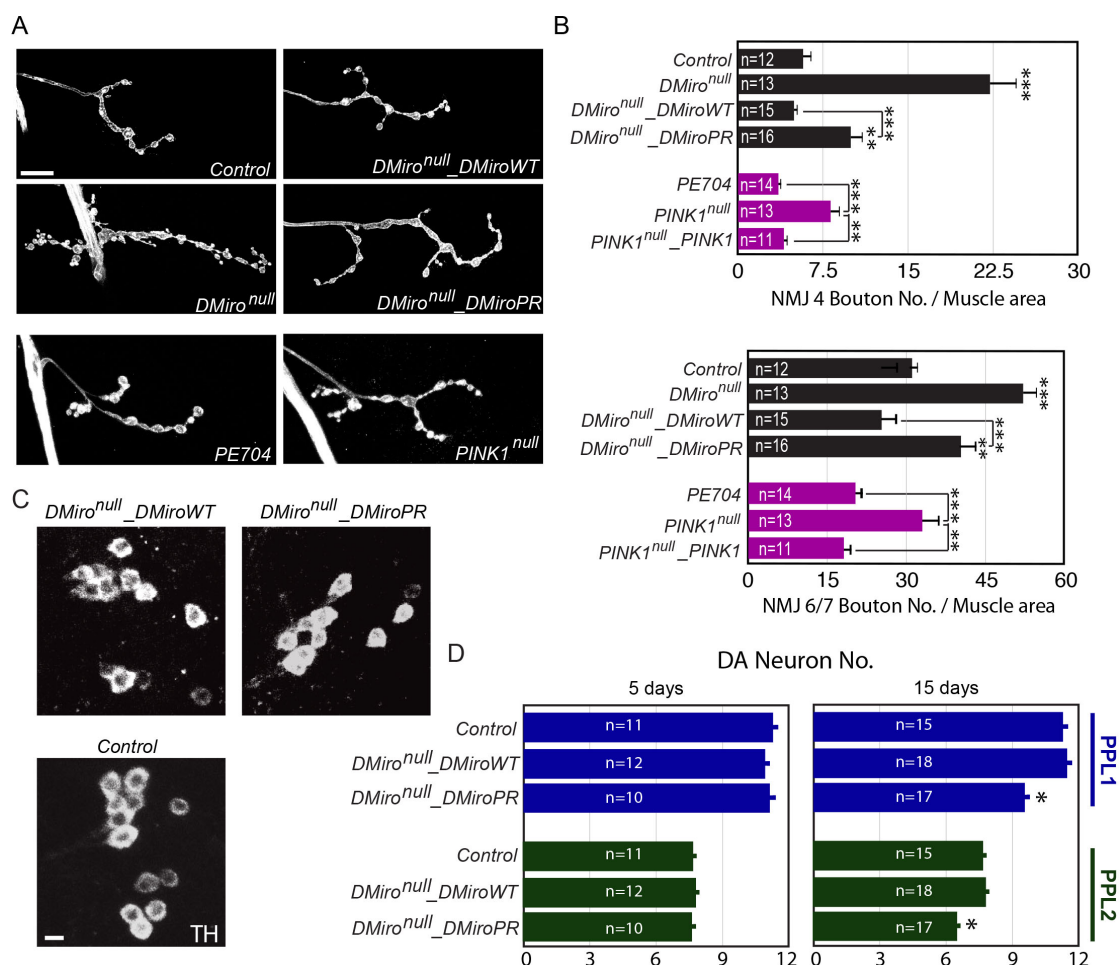
Figure 5 | DMiro^{S182A,S324A,T325A} or Loss of PINK1 Causes Synaptic Overgrowth and DA Neurodegeneration. (A) NMJ boutons visualized by anti-HRP at muscle 4 hemisegment A2 of third instar larvae. (B) Quantification of the type Ib bouton number normalized to the muscle size at muscle 4 hemisegment A2 shown in (A), or at muscle 6/7 hemisegment A2. n = 11–16 larvae. (C) The PPL1 clusters of DA neurons visualized by anti-TH in adult brains 15 days after eclosion. (D) Quantification of the number of DA neurons in one PPL1 or PPL2 cluster per brain of adult flies of 15 days after eclosion shown in (C), or of 5 days after eclosion. n = 10–18 brains. Scale bars: (A) 50 μm; (C) 5 μm.
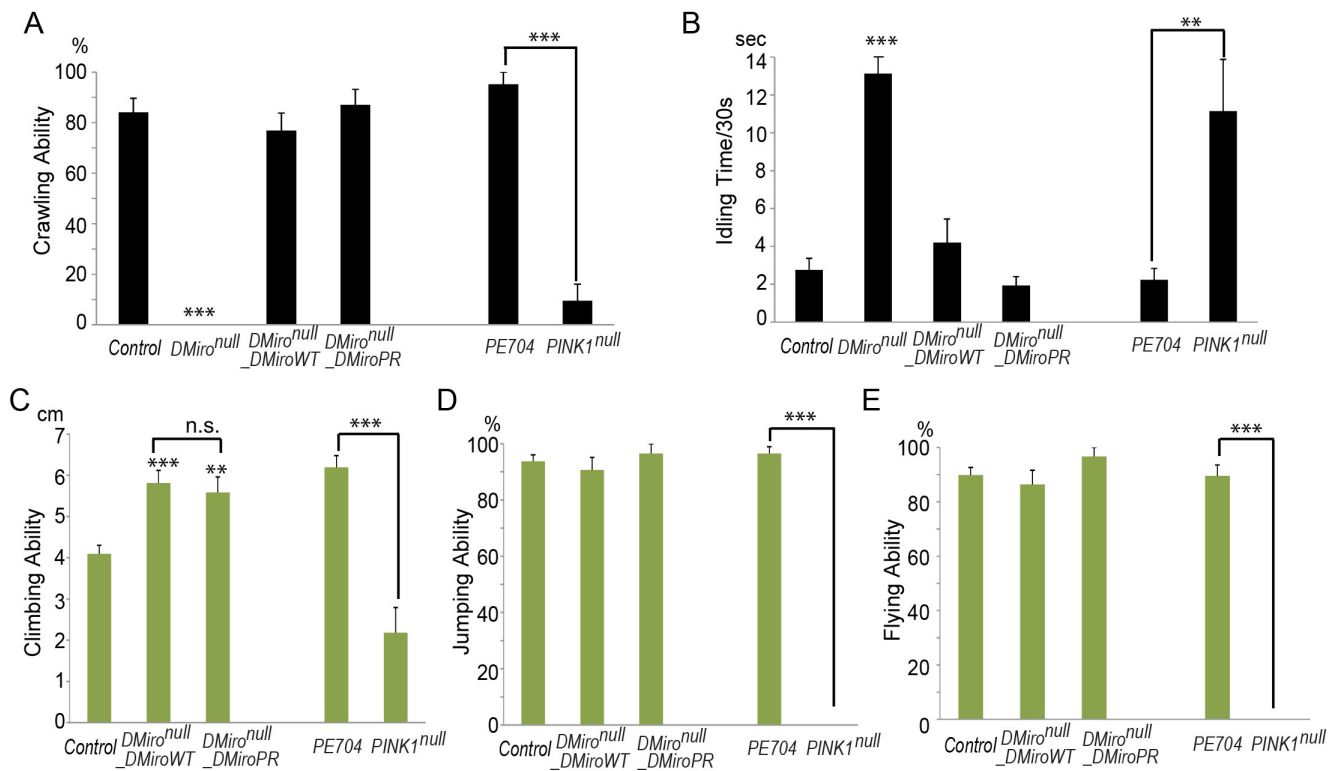
Figure 6 | Ser182, Ser324, and Thr325 of DMiro Do Not Mediate Locomotor and Flight Abilities in Larvae and Adult Flies. Crawling ability (*A*), and idling time in 30 sec (*B*), of third instar larvae with different genotypes were quantified. n = 21–44. Climbing (*C*), jumping (*D*), and flying (*E*) abilities of adult flies 15 days after eclosion were quantified. n = 22–119.

Discussion

Although several phosphorylation substrates of the mitochondrial Ser/Thr kinase PINK1 have been identified, the precise functional consequences of PINK1-mediated phosphorylation *in vivo* remain unclear. Here we report that in *Drosophila* PINK1 may inhibit mitochondrial movement and synaptic growth at larval NMJs, and protect DA neurons in adult brains, by phosphorylating the atypical GTPase DMiro.

Drosophila is a robust genetic and cellular tool for modeling human neurodegenerative diseases. Loss of PINK1 in *Drosophila* mimics many aspects of PD pathology, including a severe loss of DA neurons, which is a hallmark of PD[31–33]. However, few of the molecular and cellular mechanisms underlying the behavioral and cellular phenotypes of *PINK1* null mutant flies have been clearly defined[30–37]. Our study identifies that DMiro[S182A,S324A,T325A], which is predicted to resist PINK1-mediated phosphorylation, causes increased mitochondrial movement, synaptic overgrowth, and loss of DA neurons. All three of these defects are also observed in *PINK1* null mutant flies ([32,33]; this study). Hence, our work suggests that Miro is a crucial substrate for causing these phenotypes by mutant PINK1. Our study opens a new door to fully dissect PINK1 functions by studying its individual substrates (Figure 7C). Since PINK1-related hereditary PD shares symptomatic and pathological similarities with the majority of idiopathic PD, such work will advance our understanding of the cellular and molecular underpinnings of PD's destructive path.

Extensive studies using cell cultures have established a critical role for PINK1 in damage-induced mitophagy[2–5]. PINK1/Parkin-dependent regulation of mitochondrial transport by controlling Miro protein levels on mitochondria is likely a key step prior to initiating mitophagy in cultured neurons[4,30]. In this study, we show that PINK1-mediated phosphorylation of DMiro is required for normal mitochondrial movement in axon terminals, synaptic growth, and the neuroprotection of DA neurons. Importantly, loss of PINK1-mediated phosphorylation of DMiro has no significant effect on the mitochondrial membrane potential, excluding the possibility that the observed phenotypic effects are due to an impairment of mitophagy and an accumulation of damaged mitochondria (Figures 3–5). Accordingly, under these conditions PINK1-mediated phosphorylation of DMiro may not be required for mitophagy. However, this does not necessarily contradict its mitophagic role; rather, this represents circumstances under which its mitophagic role is dispensable. It is tempting to speculate that an efficient regulation of mitophagy is more critical in aging neurons.

Our studies identify a conserved site in human and *Drosophila* Miro, MiroSer156/DMiroSer182, to be a main residue for PINK1-mediated phosphorylation ([4] and this study). We also find additional conserved sites in *DMiro* that may have a cooperative role (Figure 1). Future studies determining their functions in mammalian systems are warranted to confirm if a similar regulatory mechanism is at play. Our study suggests that these PINK1 phosphorylation sites in DMiro are not absolutely required for the subsequent Parkin-dependent degradation of DMiro, because when harsh treatment of CCCP is applied, the phospho-resistant DMiro[S182A,S324A,T325A] is degraded (Figure 1C, D). The failure of DMiro[S182A,S324A,T325A] to prevent degradation under this condition might be due to PINK1-mediated phosphorylation on other sites that promote DMiro degradation, or due to activation of additional mechanisms. In two recent studies, Miro[S156A] is significantly degraded by co-expression of PINK1 and Parkin in addition to CCCP treatment in Hela cells[30], or by overexpression of Parkin together with Carbonyl cyanide 4-(trifluoromethoxy) phenylhydrazone (FCCP, another mitochondrial uncoupler) treatment in SH-SY5Y cells[38]; whereas in our previous study, Miro[S156A] is resistant to degradation when only PINK1 or Parkin is individually expressed in HEK293T cells[4]. This again suggests that if the PINK1/Parkin pathway is overwhelmingly activated, mutating the few known PINK1-mediated phosphorylation residues in Miro is not sufficient to prevent its degradation.
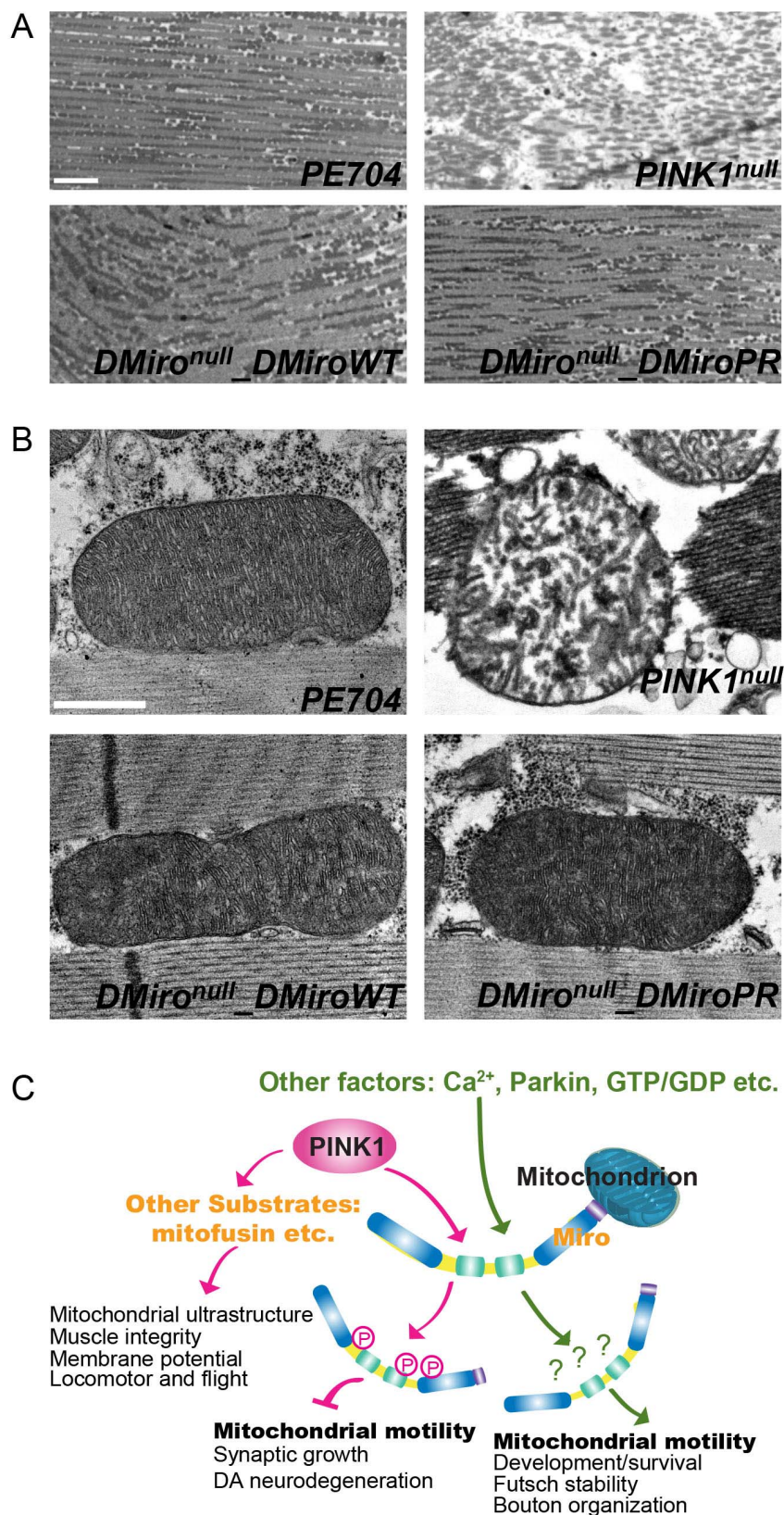
Figure 7 | DMiro^{S182A,S324A,T325A} Does Not Cause Muscle Degeneration or Swollen Mitochondria. (*A*) Light microscopic images of thick sections show indirect flight muscles, and (*B*) TEM images of thin sections show mitochondria inside muscle cells, performed on thoraces of adult flies as indicated 5 days after eclosion. (*C*) Schematic representation of the regulatory mechanisms by which PINK1 and Miro control cellular functions. Blue boxes in Miro indicate GTPase domains and green boxes are EF-hands. Scale bars: (*A*) 10 μm; (*B*) 0.5 μm.

Why is mitochondrial motility increased in "DMiro^{null}, da > DMiro^{S182A,S324A,T325A}" (Figure 4)? DMiro^{S182A,S324A,T325A} is resistant to PINK1/Parkin-mediated degradation (Figure 1), which may lead to more DMiro^{S182A,S324A,T325A} accumulation on mitochondria. Unexpectedly, DMiro^{S182A,S324A,T325A} protein level in "DMiro^{null}, da > DMiro^{S182A,S324A,T325A}" is not significantly upregulated as compared with DMiro^{wildtype} in "DMiro^{null}, da > DMiro^{wildtype}" using fly whole body lysates (Figure 2B). It is likely that PINK1/Parkin-dependent degradation of Miro only occurs in certain cell types, at certain sub-cellular locations, on certain populations of mitochondria, or under certain circumstances, and thus it is hard to detect a dramatic change using whole body lysates or without overexpression of PINK1/Parkin. Future mechanistic study is needed to test these hypotheses, such as detecting Miro subcellular localization and expression levels in different cell types, in different developmental stages, and with different mitochondrial stresses.

Our work highlights the importance of a precise control of mitochondrial movement for neuronal health. Anterograde mitochondrial transport in axons is mediated by a conserved motor/adaptor complex, which includes the motor kinesin heavy chain (KHC), the adaptor protein milton and the mitochondrial membrane anchor Miro[13–18]. In the current model, Miro binds to milton, which in turn binds to KHC recruiting mitochondria to the motors and microtubules[10,11]. In addition to the transmembrane domain inserted into the OMM, Miro features a pair of EF-hands and two GTPase domains[15]. Miro was also recently found to be a substrate of the Ser/Thr kinase PINK1[4] and of the E3 ubiquitin ligase Parkin[39,40], both mutated in PD. Thus, mitochondrial transport can be regulated by multiple signals upstream of Miro and the motor complex maintaining energy and Ca^{2+} homeostasis in neuronal processes and terminals. For example, loss of PINK1-mediated phosphorylation of DMiro increases local mitochondrial movement at NMJs (Figure 4). In turn, this may disrupt synaptic homeostasis leading to synaptic overgrowth (Figure 5) by mechanisms yet to be identified. Similarly, the loss of DA neurons in adult brains (Figure 5) could well be a consequence of impaired synaptic homeostasis together with an accumulation of dysfunctional mitochondria. Local signals that regulate mitochondrial transport through Miro must be crucial to supporting neuronal functions (Figure 7C). Our study elucidates a fundamental biological mechanism demanded by a healthy neuron.

Methods

Fly stocks. The following fly stocks were used: da-GAL4, CCAP-GAL4[4], Actin-GAL4, DMiro^{sd26} [19], DMiro^{sd32} [19], PE704[31] and PINK1^5 [31]. UAS-T7-DMiro^{wildtype}, UAS-T7-DMiro^{S182A,S324A,T325A} and UAS-PINK1-Flag flies were generated using the PhiC31 integrase-mediated transgenesis system, with insertion at an estimated position of 25C6 at the attP40 site (BestGene Inc.)[41].

Constructs. Phospho-resistant mutations of DMiro were first generated in pA1-T7-DMiro[4] using site-directed mutagenesis (Stratagene). Wildtype and mutant T7-DMiro cDNA was then amplified by PCR engineered with KpnI/XbaI restriction sites at either side, and cut (New England BioLabs) and re-ligated into a pUASTattB vector[42]. PINK1-Flag cDNA was amplified by PCR engineered with BglII/XbaI restriction sites at either side from the pcDNA3.1-PINK1-Flag[4], and cut (New England BioLabs) and re-ligated into a pUASTattB vector. All the constructs were confirmed by sequencing. pEYFP-Parkin[43] was used as described[4].

Cell Culture and Western Blotting. HEK293T cells were cultured, transfected and lysed, and adult flies were lysed, as previously described[14,44]. Lysates were analyzed by SDS-PAGE and immunoblotted with rabbit anti-GFP (Invitrogen) at 1:5000, mouse anti-T7 (Novagen) at 1:10000, mouse anti-ATP5β (AbCam) at 1:5000, guinea pig anti-DMiro (GP5) at 1:20000, or mouse anti-tubulin (Sigma) at 1:3000, and Cy5-conjugated-goat anti-rabbit or mouse IgG (GE Healthcare) at 1:5000, or HRP-conjugated-goat anti-rabbit, guinea pig or mouse IgG (Jackson ImmunoResearch Laboratories) at 1:3000. For quantitative western blotting (Figure 1), immunoblots were scanned by a STORM 860 fluorimager (Amersham BioSciences).

Live Image Acquisition and Quantification. Third instar wandering larvae were dissected in Schneider's medium (Sigma) with 5 mM EGTA at 22°C in a chamber on a glass slide[4], and then washed and incubated for 10 min with fresh Schneider's medium with 5 mM EGTA, 10 μM JC1 (Life Technologies), and Alexa 647-conjugated-goat anti-HRP (Jackson ImmunoResearch Laboratories) at 1:50. Larvae

were subsequently washed 3 times and kept in Schneider's medium with 5 mM EGTA for live imaging. For Figure 3C, intensity of accumulative mitochondrial JC1 excited at 488 nm and emitted at 570–625 nm was normalized to that of diffuse cytoplasmic JC1 excited at 488 nm and emitted at 500–554 nm, from the same axonal region. For Figure 4, accumulative mitochondrial JC1 fluorescence or GFP was excited by a mercury lamp (HBO100), and images were captured every 2 sec using a Leica DFC365 FX CCD camera for SPE II system with a Leica N2.1 filter LP 590 nm or an I3 filter LP 515 nm (JH Technologies). For NMJ images with JC1, the time-lapse images at 0 sec and 20 sec were pseudo-colored by red and green respectively and merged. The overlapped area (full yellow area, defined by a single 8-bit byte integer number of 255 of green and red, but 0 of blue), of the image was subtracted. The remaining green and red pixels were split again into two images. Non-overlapping/total JC1 pixel ratio was calculated as {(intensity of red pixels after subtraction/intensity of red pixels before subtraction) + (intensity of green pixels after subtraction/intensity of green pixels before subtraction)}/2. For axonal images with CCAP > mito-GFP, kymographs were generated and analyzed as previously described[4]. All images were processed with Adobe Photoshop CS4 or NIH ImageJ using only linear adjustments of contrast and brightness.

Immunocytochemistry and Confocal Microscopy. Third instar wandering larvae or adult brains were dissected in PBS or PBT (0.3% Tween 20 in PBS), and incubated with fixative solution (4% formaldehyde in PBT) for 20 min, and immunostained with mouse anti-Futsch (Developmental Studies Hybridoma Bank) at 1:100 or mouse anti-TH (EMD Millipore Corporation) at 1:200 and Alexa 488-conjugated-goat anti-mouse IgG (Jackson ImmunoResearch Laboratories) at 1:500, or TRITC-conjugated-rabbit anti-HRP (Jackson ImmunoResearch Laboratories) at 1:100. Samples were imaged at room temperature (22°C) with a 20×/N.A.0.60 or a 63×/N.A.1.30 oil Plan-Apochromat objective on a Leica SPE laser scanning confocal microscope (JH Technologies), with identical imaging parameters among different genotypes in a blind fashion. For Figures 2C and 5B, the area of muscle 4 or 6/7 was measured and calculated under a Leica DFC365 FX CCD camera with brightfield 20× magnification. Images were processed with Photoshop CS4 using only linear adjustments of contrast and color.

Generation of a DMiro Antibody. An N-terminally His-tagged DMiro-RC cDNA fragment (residues 1–590, pET100 TOPO vector) was expressed in BL21 (DE3) E. coli cells, and purified under denaturing condition using Ni-TED agarose by a standard protocol (Affymetrix, Cleveland, OH). Guinea pig polyclonal antibodies were generated using a standard 60-day injection protocol (Cocalico Biologicals, Reamstown, PA). The specificity of the polyclonal sera (anti-DMiro GP5) was verified by western blots and immunostainings using DMiro null mutations.

Detection of ATP Level. The larval ATP level was measured using a luciferase-based bioluminescence assay (ATP Determination Kit, Life Technologies). For each experiment, third instar larvae were homogenized in 100 μl lysis buffer (6 M quinidine-HCl, 100 M Tris pH8.0, and 4 mM EDTA). The lysates were boiled for 5 min, placed on ice for 5 min, and centrifuged at 20,000 g for 15 min. The supernatant was then diluted to 1:1000 with reaction buffer (provided by the kit) and luciferase was added for 1 min at 25°C. The luminescence was immediately measured using a Glomax Multi Jr. Reader (Promega). Each reading was normalized to the corresponding protein concentration measured by a bicinchoninic acid (BCA) assay (Thermo Scientific).

Behavioral Assays. Crawling ability was defined as the ability of the larva to move from the middle of a 55 mm grape agar plate to halfway to the edge (13.75 mm) in 30 sec. If the larva was able to do this, it was scored as a 1, and if it was not, it was scored as a 0; crawling ability was given as a percentage of total larvae that scored a 1. Idling time was defined as the amount of time the larva spent not moving in 30 sec. Climbing ability was defined as the distance the fly climbed in 5 sec. Jumping ability was defined as the ability of the fly to respond to being tapped in a petri dish, by jumping to right itself. Flying ability was defined as the ability of the fly to fly when the dish was turned upside down at 20 cm above a bench. For jumping and flying, if the fly was able to perform the action, it was scored as a 1, and if not, it was scored as a 0; ability was given as a percentage of total flies that scored a 1.

Transmission Electron Microscopy (TEM). Dissected adult thoraces were fixed in modified Trump's fixative (0.1 M sodium cacodylate buffer, 1% glutaraldehyde, and 4% formaldehyde) at room temperature (22°C) for 30 min, and then at 4°C overnight. The fixed specimens were rinsed three times in 0.1 M sodium cacodylate buffer for 10 min, post-fixed with 2% osmium tetroxide in 0.1 M sodium cacodylate buffer for 30 min, rinsed three times in 0.1 M sodium cacodylate buffer for 10 min, and finally rinsed five times in ddH$_2$O for 10 min. The specimens were then stained en bloc with 2% aqueous uranyl acetate for 20 min, dehydrated in a graded ethanol series, and subsequently set into Spurr's embedding medium. Thin sections (90 nm) were stained with uranyl acetate and lead citrate, and imaged with a TEM1230 electron microscope (JEOL Company) and a 967 slow-scan, cooled CCD camera (Gatan). TEM images were processed with Photoshop CS4.

Statistical Analysis. Throughout this paper, the distribution of data points is expressed as mean ± standard error of the mean (S.E.M.). Mann-Whitney U test was used for statistical comparisons between two groups, and One-Way ANOVA

Post-Hoc Tukey test was performed for comparisons among multiple groups. Manual quantification was performed in a blind fashion.

1. Valente, E. M. et al. Hereditary early-onset Parkinson's disease caused by mutations in PINK1. Science 304, 1158–1160, doi:10.1126/science.1096284 (2004).
2. Narendra, D., Walker, J. E. & Youle, R. Mitochondrial quality control mediated by PINK1 and Parkin: links to parkinsonism. Cold Spring Harb. Perspect. Biol. 4, doi:10.1101/cshperspect.a011338 (2012).
3. Vives-Bauza, C., de Vries, R. L., Tocilescu, M. & Przedborski, S. PINK1/Parkin direct mitochondria to autophagy. Autophagy 6, 315–316 (2010).
4. Wang, X. et al. PINK1 and Parkin target Miro for phosphorylation and degradation to arrest mitochondrial motility. Cell 147, 893–906, doi:10.1016/j.cell.2011.10.018 (2011).
5. Whitworth, A. J. & Pallanck, L. J. The PINK1/Parkin pathway: a mitochondrial quality control system? J. Bioenerg. Biomembr. 41, 499–503, doi:10.1007/s10863-009-9253-3 (2009).
6. Sha, D., Chin, L. S. & Li, L. Phosphorylation of parkin by Parkinson disease-linked kinase PINK1 activates parkin E3 ligase function and NF-kappaB signaling. Hum. Mol. Gen. 19, 352–363, doi:10.1093/hmg/ddp501 (2010).
7. Kim, Y. et al. PINK1 controls mitochondrial localization of Parkin through direct phosphorylation. Biochem. Biophys. Res. Commun. 377, 975–980, doi:10.1016/j.bbrc.2008.10.104 (2008).
8. Kondapalli, C. et al. PINK1 is activated by mitochondrial membrane potential depolarization and stimulates Parkin E3 ligase activity by phosphorylating Serine 65. Open Biol. 2, 120080, doi:10.1098/rsob.120080 (2012).
9. Shiba-Fukushima, K. et al. PINK1-mediated phosphorylation of the Parkin ubiquitin-like domain primes mitochondrial translocation of Parkin and regulates mitophagy. Sci. Rep. 2, 1002, doi:10.1038/srep01002 (2012).
10. Kane, L. A. et al. PINK1 phosphorylates ubiquitin to activate Parkin E3 ubiquitin ligase activity. J. Cell Biol. 205, 143–153, doi:10.1083/jcb.201402104 (2014).
11. Kazlauskaite, A. et al. Parkin is activated by PINK1-dependent phosphorylation of ubiquitin at Ser65. Biochem. J. 460, 127–139, doi:10.1042/BJ20140334 (2014).
12. Koyano, F. et al. Ubiquitin is phosphorylated by PINK1 to activate parkin. Nature 510, 162–166, doi:10.1038/nature13392 (2014).
13. Glater, E. E., Megeath, L. J., Stowers, R. S. & Schwarz, T. L. Axonal transport of mitochondria requires milton to recruit kinesin heavy chain and is light chain independent. J. Cell Bio. 173, 545–557, doi:10.1083/jcb.200601067 (2006).
14. Wang, X. & Schwarz, T. L. The mechanism of Ca2+ -dependent regulation of kinesin-mediated mitochondrial motility. Cell 136, 163–174, doi:10.1016/j.cell.2008.11.046 (2009).
15. Fransson, S., Ruusala, A. & Aspenstrom, P. The atypical Rho GTPases Miro-1 and Miro-2 have essential roles in mitochondrial trafficking. Biochem. Biophys. Res. Commun. 344, 500–510, doi:10.1016/j.bbrc.2006.03.163 (2006).
16. van Spronsen, M. et al. TRAK/Milton motor-adaptor proteins steer mitochondrial trafficking to axons and dendrites. Neuron 77, 485–502, doi:10.1016/j.neuron.2012.11.027 (2013).
17. Koutsopoulos, O. S. et al. Human Miltons associate with mitochondria and induce microtubule-dependent remodeling of mitochondrial networks. Biochim. Biophys. Acta 1803, 564–574, doi:10.1016/j.bbamcr.2010.03.006 (2010).
18. Macaskill, A. F. et al. Miro1 is a calcium sensor for glutamate receptor-dependent localization of mitochondria at synapses. Neuron 61, 541–555, doi:10.1016/j.neuron.2009.01.030 (2009).
19. Guo, X. et al. The GTPase dMiro is required for axonal transport of mitochondria to Drosophila synapses. Neuron 47, 379–393, doi:10.1016/j.neuron.2005.06.027 (2005).
20. Chen, Y. & Dorn, G. W., 2nd. PINK1-phosphorylated mitofusin 2 is a Parkin receptor for culling damaged mitochondria. Science 340, 471–475, doi:10.1126/science.1231031 (2013).
21. Karbowski, M. & Youle, R. J. Regulating mitochondrial outer membrane proteins by ubiquitination and proteasomal degradation. Curr. Opin. Cell Biol. 23, 476–482, doi:10.1016/j.ceb.2011.05.007 (2011).
22. Poole, A. C. et al. The PINK1/Parkin pathway regulates mitochondrial morphology. Proc. Natl. Acad. Sci. U.S.A. 105, 1638–1643, doi:10.1073/pnas.0709336105 (2008).
23. Poole, A. C., Thomas, R. E., Yu, S., Vincow, E. S. & Pallanck, L. The mitochondrial fusion-promoting factor mitofusin is a substrate of the PINK1/parkin pathway. PLOS One 5, e10054, doi:10.1371/journal.pone.0010054 (2010).
24. Tanaka, A. et al. Proteasome and p97 mediate mitophagy and degradation of mitofusins induced by Parkin. J. Cell Biol. 191, 1367–1380, doi:10.1083/jcb.201007013 (2010).
25. Yang, Y. et al. Pink1 regulates mitochondrial dynamics through interaction with the fission/fusion machinery. Proc. Natl. Acad. Sci. U.S.A. 105, 7070–7075, doi:10.1073/pnas.0711845105 (2008).
26. Ziviani, E., Tao, R. N. & Whitworth, A. J. Drosophila parkin requires PINK1 for mitochondrial translocation and ubiquitinates mitofusin. Proc. Natl. Acad. Sci. U.S.A. 107, 5018–5023, doi:10.1073/pnas.0913485107 (2010).
27. Arena, G. et al. PINK1 protects against cell death induced by mitochondrial depolarization, by phosphorylating Bcl-xL and impairing its pro-apoptotic cleavage. Cell Death Differ. 20, 920–930, doi:10.1038/cdd.2013.19 (2013).
28. Pridgeon, J. W., Olzmann, J. A., Chin, L. S. & Li, L. PINK1 protects against oxidative stress by phosphorylating mitochondrial chaperone TRAP1. PLoS Biol. 5, e172, doi:10.1371/journal.pbio.0050172 (2007).
29. Plun-Favreau, H. et al. The mitochondrial protease HtrA2 is regulated by Parkinson's disease-associated kinase PINK1. Nat. Cell Biol. 9, 1243–1252, doi:10.1038/ncb1644 (2007).
30. Liu, S. et al. Parkinson's disease-associated kinase PINK1 regulates Miro protein level and axonal transport of mitochondria. PLoS Genet. 8, e1002537, doi:10.1371/journal.pgen.1002537 (2012).
31. Clark, I. E. et al. Drosophila pink1 is required for mitochondrial function and interacts genetically with parkin. Nature 441, 1162–1166, doi:10.1038/nature04779 (2006).
32. Park, J. et al. Mitochondrial dysfunction in Drosophila PINK1 mutants is complemented by parkin. Nature 441, 1157–1161, doi:10.1038/nature04788 (2006).
33. Yang, Y. et al. Mitochondrial pathology and muscle and dopaminergic neuron degeneration caused by inactivation of Drosophila Pink1 is rescued by Parkin. Proc. Natl. Acad. Sci. U.S.A. 103, 10793–10798, doi:10.1073/pnas.0602493103 (2006).
34. Imai, Y. et al. The loss of PGAM5 suppresses the mitochondrial degeneration caused by inactivation of PINK1 in Drosophila. PLoS Genet. 6, e1001229, doi:10.1371/journal.pgen.1001229 (2010).
35. Vilain, S. et al. The yeast complex I equivalent NADH dehydrogenase rescues pink1 mutants. PLoS Genet. 8, e1002456, doi:10.1371/journal.pgen.1002456 (2012).
36. Vos, M. et al. Vitamin K2 is a mitochondrial electron carrier that rescues pink1 deficiency. Science 336, 1306–1310, doi:10.1126/science.1218632 (2012).
37. Hao, L. Y., Giasson, B. I. & Bonini, N. M. DJ-1 is critical for mitochondrial function and rescues PINK1 loss of function. Proc. Natl. Acad. Sci. U.S.A. 107, 9747–9752, doi:10.1073/pnas.0911175107 (2010).
38. Birsa, N. et al. K27 ubiquitination of the mitochondrial transport protein Miro is dependent on serine 65 of the Parkin ubiquitin ligase. J. Biol. Chem. 289, 14569–14582, doi:10.1074/jbc.M114.563031 (2014).
39. Chan, N. C. et al. Broad activation of the ubiquitin-proteasome system by Parkin is critical for mitophagy. Hum. Mol. Gen. 20, 1726–1737, doi:10.1093/hmg/ddr048 (2011).
40. Sarraf, S. A. et al. Landscape of the PARKIN-dependent ubiquitylome in response to mitochondrial depolarization. Nature 496, 372–376, doi:10.1038/nature12043 (2013).
41. Markstein, M., Pitsouli, C., Villalta, C., Celniker, S. E. & Perrimon, N. Exploiting position effects and the gypsy retrovirus insulator to engineer precisely expressed transgenes. Nat. Genet. 40, 476–483, doi:10.1038/ng.101 (2008).
42. Groth, A. C., Fish, M., Nusse, R. & Calos, M. P. Construction of transgenic Drosophila by using the site-specific integrase from phage phiC31. Genetics 166, 1775–1782 (2004).
43. Narendra, D., Tanaka, A., Suen, D. F. & Youle, R. J. Parkin-induced mitophagy in the pathogenesis of Parkinson disease. Autophagy 5, 706–708 (2009).
44. Tsai, P. I. et al. Activity-dependent retrograde laminin A signaling regulates synapse growth at Drosophila neuromuscular junctions. Proc. Natl. Acad. Sci. U.S.A. 109, 17699–17704, doi:10.1073/pnas.1206416109 (2012).

Acknowledgments

Author contributions

J.L. and X.W. prepared Figure 1, P.I. prepared Figure 2, 3, 4, 5, 7, M.C. prepared Figure 6 and helped with fly crossing, M.B. and K.Z. made antibodies, C.H. provided help for cell culture and biochemistry, X.W., P.I., M.C. and K.Z. wrote the manuscript. All authors reviewed and approved the manuscript.

Additional information